

From superconductivity near a quantum phase transition to superconducting graphite

S S Saxena¹, K Ahilan¹, T E Weller², M Ellerby², R P Smith¹, N T Skipper²,
S Rowley¹, A Kusmartseva¹ and G G Lonzarich¹

1. Cavendish Laboratory, University of Cambridge, Madingley Road, Cambridge CB3 0HE, UK

2. Department of Physics and Astronomy, University College of London, Gower Street, London WC1E 6BT, UK

(Received 10 July 2006; accepted 15 September 2006)

Abstract

The collapse of antiferromagnetic order as a function of some quantum tuning parameter such as carrier density or hydrostatic pressure is often accompanied by a region of superconductivity. The corresponding phenomenon in the potentially simpler case of itinerant-electron ferromagnetism, however, remains more illusive. In this paper we consider the reasons why this may be so and summarize evidence suggesting that the obstacles to observing the phenomenon are apparently overcome in a few metallic ferromagnets. A new twist to the problem presented by the recent discoveries in ferroelectric symmetric systems and new graphite intercalate superconductors will also be discussed.

Keywords: strongly correlated electrons, superconductivity, magnetism, ferroelectricity, intercalated graphite, quantum phase transitions

1. Introduction

This paper focuses on understanding the nature of quantum order in low temperatures. In recent years this area of research has led to the study of (i) novel metallic states not described by Fermi liquid theory, (ii) anisotropic types of electron-electron and electron-hole pair condensates, (iii) quantum critical phenomena, (iv) quantum critical ferroelectrics and (v) elevated temperature superconductivity in graphite intercalates.

The crossover from ferromagnetism or antiferromagnetism to paramagnetism as a function of a 'quantum' control parameter such as pressure has turned out to be a much more subtle and interesting problem than was originally imagined in the early days of our field. On the border of long-range magnetic order one expects several quantum states of more or less exotic nature to be nearly degenerate. Minute metallurgical or environmental changes can induce transitions between these states and give rise to complex behaviour that, in extreme cases, could be called 'adaptive'.

Our research has focused on the investigation of the temperature-pressure phase diagram on the border of magnetism in relatively simple stoichiometric compounds of high purity in which well-defined forms of quantum order might be observed.

This approach has led us to the discovery of an

unusual kind of superconductivity that survives only in a very narrow window of pressure close to the boundary of antiferromagnetism in CePd_2Si_2 and CeIn_3 (Figure 1) [15,19]. This phenomenon - reproduced in many laboratories across the world and confirmed by calorimetric studies to be bulk in nature [36,38]-was anticipated by some of us in terms of the effects of spin fluctuations. Contrary to widely held views, the spin fluctuations are not in general pair breaking on the edge of magnetism, but can, under suitable circumstances, form robust Cooper pairs [3, 31, 52].

Analysis by Monthoux and Lonzarich suggested that an order-of-magnitude increase in the superconducting transition temperature might be achieved if cubic CeIn_3 could be deformed into an anisotropic, quasi-2D structure [3]. This prediction led to the study of the tetragonal relatives of CeIn_3 , which were indeed found to exhibit more strongly bound pairs. Interestingly this way of thinking provided the basis for discovery of elevated temperature superconductivity in an entirely new class of materials, namely, graphite intercalates C_6Ca and C_6Yb where superconductivity is not related to magnetism but is mediated by a novel electronic state of Carbon [37, 47, 60, 61].

We also suggested that a different kind of anisotropy, namely, uniaxial magnetic anisotropy, should increase

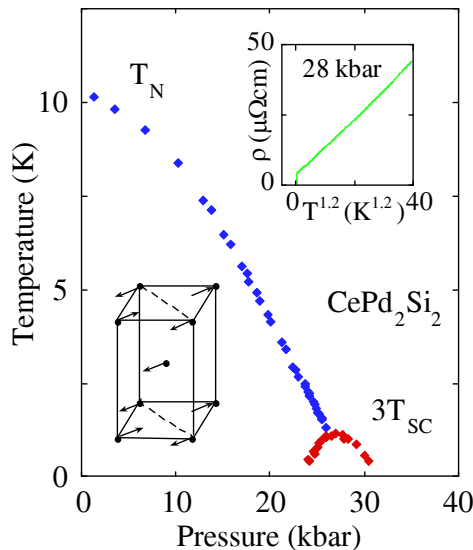


Figure 1. (color online) Unconventional normal and superconducting states on the border of metallic antiferromagnetism. Superconductivity is observed in pure crystals of CePd_2Si_2 below T_{SC} near the critical pressure where the Neel temperature T_N vanishes. The normal state above T_{SC} is characterised by an anomalous resistivity that varies as $T^{1.2 \pm 0.1}$ over two decades in temperature (inset gives resistivity along the a-axis). (After ND Mathur, *et al.*, *Nature* **394** (1998) 39) [19].

the likelihood of detecting the long-sought-after superconductivity on the border of ferromagnetism [3]. This insight led Cambridge-Grenoble team, to the discovery of the first example of superconductivity in an itinerant-electron ferromagnet, UGe_2 [16] (Figure 2), which exhibits an exchange-split Fermi surface reminiscent of that observed in d-metal ferromagnets such as Fe, Co and Ni [20, 59]. This finding, too, was confirmed to be a bulk effect [32] and was soon followed by related discoveries in (i) the ferromagnetic state of URhGe [40] and UIr and (ii) the paramagnetic state of Fe [16, 41] close to the ferromagnetic boundary at very high pressures.

There is growing evidence that the above systems may represent essentially a new class of superconductors that has become a point of focus in laboratories worldwide (Ref. 3 and papers cited therein).

Where superconductivity on the border of magnetism is absent one observes metallic states that cannot be described fully in terms of the standard theory of metals or in terms of existing theories of quantum phase transitions [20, 35, 51]. It is interesting to note that, however, the theory of quantum critical phenomena works much better in the case of ferroelectric and nearly ferroelectric systems and this has allowed us to embark on a totally new avenue of research with much broader implications [63, 64].

The above research benefited from our development of novel pressure cells [17] and of a magnetic refrigerator designed for ease-of-use, low cost and wide temperature sweeps (40 mK-290 K).

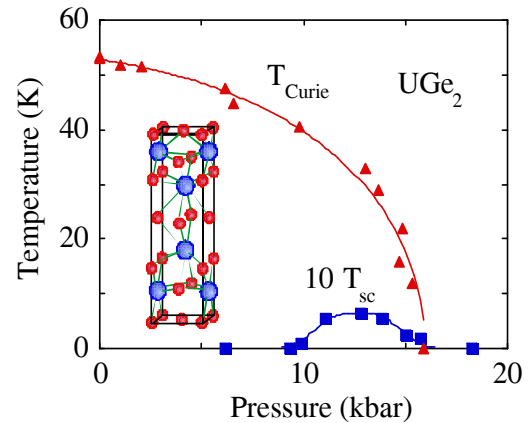


Figure 2. (color online) Unconventional superconductivity in an itinerant-electron ferromagnet. There is growing evidence that the superconducting state observed in UGe_2 in the spin-polarized side of the ferromagnetic boundary is associated with electron pairing in the spin-triplet state. Not shown is an additional phase transition line that intersects the peak of the superconducting dome. (After SS Saxena, *et al.*, *Nature* **406** (2000) 587) [16].

1.1 Background

This field has been guided in part by the spin-fluctuation model of itinerant-electron magnetism. The conceptual basis of this model was introduced in the 1960s and 1970s by Schrieffer, Doniach, Moriya, Hertz and others, extended for quantitative comparison with experiments by Lonzarich and others in the 1980s, and put into its modern form by Millis in the 1990s [20, 51, 55, 58]. The early investigations of the Fermi surface and of paramagnons in nearly magnetic metals together with the theoretical analyses showed for the first time that the spin fluctuation model could be tested quantitatively [20, 27-29]. The natural extension of this model to the problem of electron pairing has provided a starting point for our most recent work [3, 31, 52]. The spin fluctuation model has demonstrated a considerable predictive power. More generally it has pointed the way to fruitful areas for experimental study and is helping us to recognise new phenomena near quantum phase transitions and beyond as in the case of new graphite superconductors and ferroelectric materials.

1.2 Novel forms of order via quantum tuning

General background

Current theory of electronically driven superconductivity makes definite predictions of the experimental conditions that are favourable for robust pairing of electrons. Some of these predictions, based on my experimental work, have recently led to a number of striking experimental discoveries in Europe, Japan and the US [16, 19, 36, 37, 44, 47, 53]. This gives one some confidence that the current theoretical framework can serve as a useful guide to the next generation of experimental research. The most dramatic prediction of the model

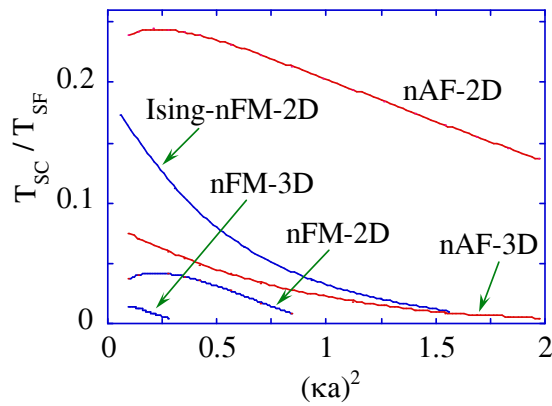


Figure 4. (color online) Calculations of T_{SC} in the magnetic pairing model for a nearly ferromagnetic (nFM) or nearly antiferromagnetic (nAF) metal in the mean field approximation (MFA) for a single band. T_{SF} is a spin-fluctuation scale and $1/(\kappa a)$ is the magnetic correlation length in units of the side of a square (2D) or cubic (3D) lattice. Corrections to MFA lead naturally to a pseudogap phenomenon at sufficiently small κ and to superconducting phase fluctuations, particularly in 2D [3].

concerns the conditions required for the observation of new robust forms of superconductivity. These conditions are normally difficult to achieve because a number of criteria need to be met simultaneously. From a practical standpoint this requires the identification of promising candidate compounds and the fine-tuning of their physical properties.

2. Superconductivity and transport on the border of metallic antiferromagnetism

2.1. Background

A number of microscopic mechanisms have been proposed for pairing of electrons in metals. On the border of magnetic long-range order one might expect that the exchange of magnetic fluctuations would typically be the dominant interaction between quasiparticles [3, 31, 52].

This magnetic interaction can lead to superconductivity in sufficiently pure specimens. The symmetry of the pairing state depends crucially on a number of factors, such as the crystal structure, the number and character of the energy bands and the nature of the incipient magnetic state. In the specific case of a nearly half-filled single-band in an orthorhombic (or higher symmetry) structure, on the border of antiferromagnetism, the model predicts a unique pairing state of d-wave symmetry. This prediction has been strikingly confirmed in the cuprates, which fulfil the above requirements [31, 52].

As in the case of the symmetry of the pairing state, the magnitude of the superconducting transition temperature T_{SC} and the transport behaviour above T_{SC} both depend sensitively on a number of materials properties. Monthoux and Lonzarich find that for the above case of a nearly-half-filled single band T_{SC} is higher for the tetragonal (quasi 2D) than a cubic (3D) lattice and for typical d-band compared with f-band

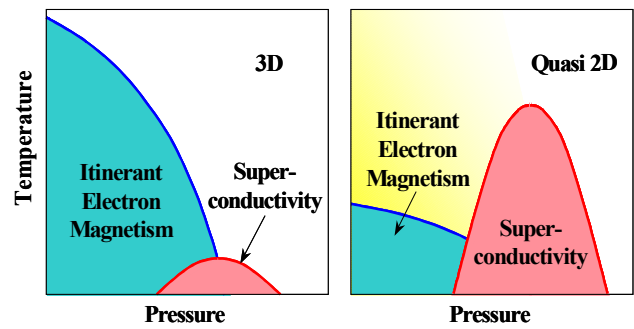


Figure 5. (color online) Schematic T-P phase diagram for the magnetic interaction model in 3D and quasi-2D on the edge of metallic antiferromagnetism [3]. The predictions are qualitatively consistent with observations in cubic $CeIn_3$ and tetragonal $CeRhIn_5$ [19, 37, 47]. A pseudogap state is expected to arise on the left of the superconducting dome in quasi-2D [3].

systems (Figure 4) [3,19]. Furthermore, the model predicts that the temperature dependence of the resistivity above T_{SC} obeys a power law with a lower exponent in quasi-2D than in 3D. In the presence of low levels of quenched disorder (relevant to practical cases of interest) the model predicts an exponent of 1 in quasi 2D and 3/2 in 3D at sufficiently low temperatures [19, 31]. The temperature range over which these exponents would be expected to be observed is much greater for typical d-band than f-band systems.

These various predictions have been interpreted in intuitive ways that have stimulated a series of experiments and discoveries broadly consistent with the magnetic interaction model. Some of the highlights are illustrated in figures 1 and 5.

Particularly striking is the comparison between the cubic antiferromagnetic metal $CeIn_3$ [19] and the closely related tetragonal compound $CeRhIn_5$ [37,47,52]. Superconductivity is found to extend over a much wider range in both temperature and pressure in $CeRhIn_5$ than in $CeIn_3$.

Moreover, the resistivity exponent above T_{SC} is close to unity in $CeRhIn_5$ and approximately 3/2 in $CeIn_3$. These findings, and the growing evidence that the symmetry of the superconducting state in $CeRhIn_5$ is d-wave, were correctly anticipated by the magnetic interaction model.

2.2 Outlook

As mentioned in the previous section, a natural consequence of the magnetic interaction model is that T_{SC} increases with electron bandwidth - or T_{SF} (see figure 4) - provided that all the other relevant parameters remain unchanged [3]. One possible way to realize this experimentally is to find d-band analogues of the above mentioned f-band compounds.

Many particularly promising d-band analogues turn out to be magnetic insulators at ambient pressure and typically are far removed from the required metallic state on the border of magnetic long-range order. A large number of these compounds have now been prepared, but have not been studied extensively perhaps partly

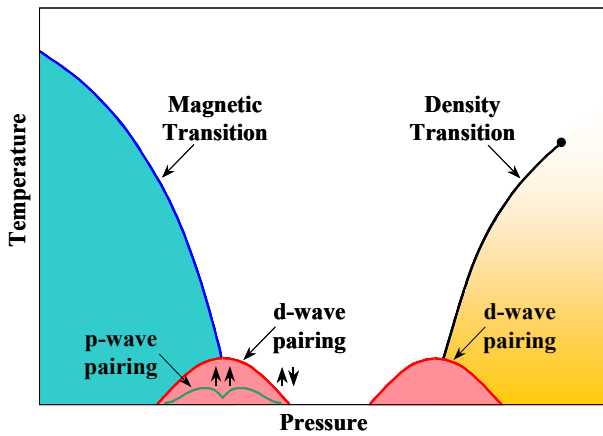


Figure 6. (color online) Extension of Figure 5 to include density as well as magnetic interactions [3, 30]. The model is qualitatively consistent with measurements in CeNi_2Ge_2 [15] and Ge-doped CeCu_2Si_2 [30]. In pure CeCu_2Si_2 [44] the superconducting domes are joined. Pairing requires adequate purity and second-order or *weakly*-first-order magnetic or density transitions.

because they cannot be metallized by conventional chemical doping methods. These systems present a major opportunity for alternative tuning methods. In many examples, we believe that the magnetic boundary can be reached by the application of hydrostatic pressure within the range attainable with current technology.

3. Pairing in itinerant-electron ferromagnetism

3.1. Background

While there have been a number of examples of superconductivity on the border of antiferromagnetism, the corresponding phenomenon on the edge of metallic ferromagnetism has, until recently, not been found. This result is not surprising within the framework of the magnetic interaction model. As shown in figure 4, for otherwise equivalent conditions the superconducting transition temperature is typically much higher on the border of antiferromagnetism than on the border of ferromagnetism. An intuitive understanding of this finding pointed to candidate systems in which superconductivity on the border of ferromagnetism would be more likely to be observed. In particular, one ought to look for systems with strong spin anisotropy, i.e., with strong spin-orbit coupling and/or in a weakly spin-polarized state (see the case 'Ising' in figure 4) [3]. This suggested a high-pressure investigation of UGe_2 , which satisfied the above conditions and could be prepared in a high purity form. UGe_2 offered the first example of the co-existence of superconductivity and itinerant-electron ferromagnetism (Figure 2) [16]. Other examples have since been found (UrhGe [40]).

3.2. Outlook

A surprising result is that superconductivity in both of the above systems has only been seen in the state with long-range ferromagnetic order and not at all in the paramagnetic state, contrary to the predictions of the original calculations shown in figure 4. One tentative

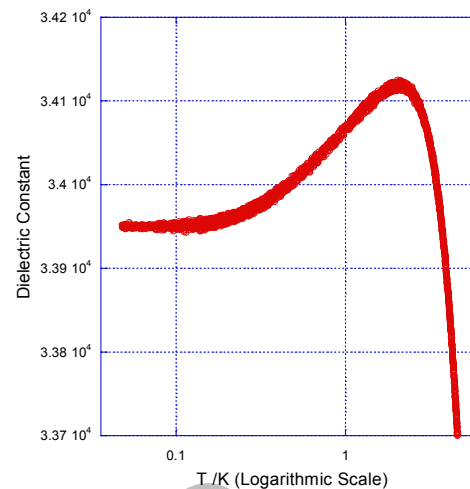


Figure 6. (color online) Low temperature dielectric constant measured down to 45mK plotted against a logarithmic temperature scale.

explanation is that superconductivity is greatly boosted by the effects of magnetic anisotropy in the spin-polarised state and is suppressed in the paramagnetic state by quenched disorder and/or the appearance of a first order magnetic phase transition. To quantify the relative robustness of superconductivity on both sides of the ferromagnetic boundary the calculations shown in figure 4 are now being extended [2].

Among the various possibilities for superconductivity on the border of magnetism, the outstanding case that is still missing, namely, superconductivity in an incipient *ferromagnet*, is that originally expected to be discovered first. This could indicate that there is a serious problem with current models. Another possibility is that the candidate materials studied thus far are (i) too far removed from the ferromagnetic boundary (e.g., because of first order magnetic transitions) or (ii) lack inversion symmetry or (iii) are too impure to support the anisotropic form of superconductivity anticipated.

4. Novel phenomena on the border of ferroelectric ordering

4.1. Background

An understanding of nearly magnetic metals is important because it is in these materials that non-Fermi-liquids arise and other behaviour such as superconductivity are observed. Here our concern is mainly with the long wavelength, small q , components of the spin density fluctuations, which are the predominant thermal excitations present. Nearly magnetic metals are well understood using the spin fluctuation model. The model can be used to understand the unusual conducting states that emerge near a QCP such as the Marginal Fermi-Liquid (MFL) expected for ZrZn_2 , Ni_3Al and other d-electron metals. Under certain circumstances, they also predict magnetically mediated superconductivity, and

have been used to understand the behaviour of itinerant heavy-fermion and copper-oxide systems.

Similarly, the nature of nearly ferroelectric materials can also be understood. Two types of ferroelectric compounds are proposed to exist. These are the well-known insulating ferroelectrics e.g. BaTiO₃ but also metallic ferroelectrics. A metallic ferroelectric is one where an internal polar axis develops just as in the case for insulating ferroelectrics. In the metallic phase however, the conduction electrons would screen out the overall electric field created by the ions. This means no external field would be detected and the characteristic FE hysteresis curves could not be measured. By 'ferroelectric metal', it is simply meant that the crystal structure has the correct group theoretical classification as is required for a ferroelectric or pyroelectric. Crudely speaking, this means that below a certain temperature T_c , the metal undergoes breaking of lattice inversion symmetry. Within the metal itself and below a certain screening length, an internal electric field would be present. Electrons travelling inside this length scale would feel the effects of the electric field, as in Cd₂Re₂O₇ and CePt₃Si.

It is of some debate whether quantum effects are present in insulating ferroelectrics. At low enough temperatures where thermal fluctuations begin to fade, the presence of any quantum fluctuations would begin to dominate. In particular, the fluctuations would be greatest in the vicinity of a quantum critical point where the particular response function or susceptibility in question diverges. When searching for such fluctuations it is therefore best to scan regions of phase space as close as possible to ferroelectric quantum critical points. At such a QCP, the speed of sound of the soft mode phonon associated with the FE transition would vanish. This is because the correlation time diverges but the correlation length can only diverge up to the physical size of the material, a few millimetres for instance.

It has been suggested that materials behaving this way could be used as model systems for studying astrophysical event horizons where the red shift factor $g_{00} = 0$ [63, 64].

4.2. Outlook

The interest in studying ferroelectrics is therefore firstly to investigate the presence of quantum effects relating to the incipient ferroelectric phase and learn about the resulting unconventional lattice state in a number of materials and over a wide range of pressures. We imagine that quantum paraelectric fluctuations may also mediate important interactions in crystals with mobile charge carriers, such as metallic ferroelectrics where superconductivity may be realised.

Our key findings so far at ambient pressure are (i) discovery of a low-temperature phase below 2K in SrTiO₃ and (ii) T² dependence of the dielectric constant between 2K and 40K due to quantum fluctuations and indicating proximity to a quantum and critical point.

We have been able to identify a number of different

compounds where we would expect to observe interesting quantum effects. These include the Perovskites SrTiO₃, KTaO₃ and BaTiO₃ as well as the GeTe family of semiconductor rock-salts. As our work confirms SrTiO₃ and KTaO₃ exist naturally very close to the quantum critical point at ambient pressure, making measurements in these compounds relatively simple.

In extreme cases, ferroelectricity can coexist with the metallic state. An example of this is found in the compound Cd₂Re₂O₇. Looking to the future, we therefore imagine that quantum ferroelectric fluctuations may mediate important interactions in crystals supporting itinerant electrons. Possible examples include oxygen reduced SrTiO₃ and the GeTe family of narrowband semiconductors. The potential for superconductivity mediated by ferroelectric waves is a real possibility.

5. Intercalated graphite systems

5.1. Background

As we have discussed in 2.1 low dimensionality is generally considered as a necessary ingredient for high superconducting transition temperatures. Surprisingly, perhaps, systems based on graphite have received little attention in this context. Introducing metal atoms between the carbon layers can tune the interlayer spacing and charging of the graphite host through a variety of electronic ground states. One such ground state is superconductivity, which is not present in pure graphite. We have discovered superconductivity in the intercalation compounds C₆Yb and C₆Ca, with transition temperatures of 6.5 and 11.5 K, respectively. These critical temperatures are unprecedented in graphitic systems and have not been explained by a simple phonon mechanism for the superconductivity. This discovery has already stimulated several proposals for the superconducting mechanism that range from coupling by way of the intercalant phonons through to acoustic plasmons. It also points towards the potential of superconductivity in systems such as carbon nanotubes.

It seems that the presence of the metal atoms between the graphite sheets allows the electrons to be conducted in a particular way. However, what is surprising is that the electronic structure calculations by our theory collaborators, Csyani et al [62], show that only the compounds where a specific interlayer electronic state of graphite is occupied by electrons become superconducting. The interlayer free electron-like state is not only a property of graphite, but also of the pure metal (these are metal bands that can be reasonably described by a weakly perturbed free electron band). It is this fortuitous combination that results in the filling of the interlayer band.

The first superconducting graphite intercalation compound to be reported [68, 69] was C₈K, which has a transition temperature of 0.15K. Interestingly, while the metastable high pressure phase C₂Li exhibits a superconducting transition at 1.9K [70], the compounds C₆Li and C₃Li are not found [67] to superconduct down to the lowest measured temperatures. In all these

compounds the transfer of charge from the metal to the graphite is thought to play an important role in the superconductivity. However, we see that there must be additional factors at work as both potassium (K) and lithium (Li) would be expected to donate one electron each to the graphite and C_8K superconducts while C_6Li does not. This non-trivial behaviour showed that the fabrication and study of different graphite intercalation compounds would be worthwhile. Therefore, we have fabricated the isostructural intercalation compounds C_6Yb and C_6Ca . Here we present results demonstrating the existence of superconductivity in these compounds together with a structural determination showing the formation of ordered structures. C_6Yb forms a hexagonal layered structure ($P6_3/mmc$) in which the intercalant atoms form a triangular array between every graphite layer (stage 1 intercalation). The alternate carbon and metal layers have an $A\alpha A\beta$ registration [7] where the A represents the carbon layers and the α and β the intercalant layers. The structure for C_6Ca has recently been refined [72] and found to differ from that of C_6Yb having a rhombohedral structure ($R-3m$), with a carbon and metal layer repeat of $A\alpha A\beta A\gamma$. The rhombohedral structure can be translated to a hexagonal basis and thus these compound may be seen in a similar light.

Two of the principle signatures of superconductivity are the absence of electrical resistivity and the development of a diamagnetic moment below the ordering transition. Figure 7 shows the results of resistivity and DC magnetisation measurements made on samples of C_6Yb and DC magnetisation measurements on C_6Ca . The results for C_6Yb (figures 7a and 7b) show a clear transition at 6.5K in the magnetization and the resistivity, both of which support the existence of superconductivity. The transition is well defined, having width of 0.2K in the resistivity. These intercalation compounds are very difficult to fabricate (see methods), nevertheless we have managed to prepare samples in which X-ray studies show that over 13% of the final volume of the sample is C_6Yb . However, field-dependent magnetization measurements made parallel to the c^* -axis of C_6Yb imply that the superconducting volume fraction is approximately 90%. This difference was resolved by scanning electron microscopy (SEM) studies which revealed that the intercalation process creates a “shell” of the intercalant with a core of pristine graphite. It is important to stress that the subsequent cleaving of several layers up to 300 μm from these samples did not remove superconductivity. The magnetization measurement shown in figure 7b, with the field of 50Oe applied parallel to the c^* -axis was performed on a disk shaped sample. The zero field cooled (ZFC) data reveals the flux expulsion and subsequent flux threading as the temperature is increased. The field cooled (FC) measurements, when compared with the ZFC result, exhibit only partial flux expulsion. In fields exceeding the superconducting upper critical field (H_{C2}) we find a weak paramagnetic signal. The origins of this

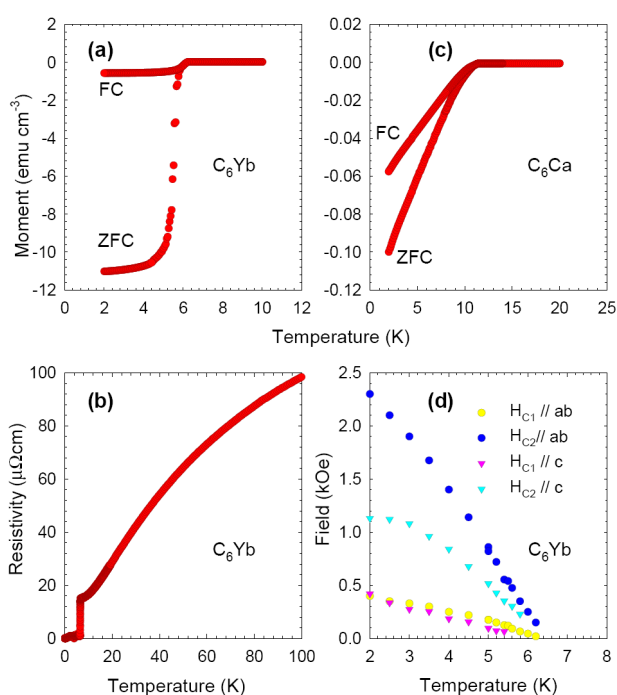


Figure 7. (color online) Temperature dependence of the magnetization and electrical resistivity for C_6Yb and C_6Ca . Magnetization measurements for C_6Yb and C_6Ca shown in (a) and (c) respectively. These measurements were made with a 50 Oe field applied parallel to the c^* -axis. These figures reveal the onset of flux expulsion in both the zero field cooled (ZFC) measurement and the field cooled (FC) measurement. The resistivity measurement for C_6Yb is shown in (b). There is a clear drop to zero resistivity indicating the existence of superconductivity. Figure 7 (d) is the superconducting phase diagram for C_6Yb . This diagram is compiled from results of the magnetization study. In both geometries the sample appears to be a type-II superconductor. There is little if any anisotropy in H_{C1} for the two geometries, whilst there is a clear anisotropy in H_{C2} .

paramagnetic moment are difficult to attribute, but we do have X-ray evidence showing a contamination of less than 1% Yb_2O_3 which is known to have an ordered moment below 2.4K [73].

The C_6Ca magnetisation results are shown in figure 7c. In the magnetization we see a clear diamagnetic onset at 11.5K in a field of 50Oe, but with no saturation of diamagnetism down to 2K. In addition, the preliminary resistivity measurements demonstrate that the resistivity goes to zero below the transition temperature. However, extreme air sensitivity and difficulties in preparation of this compound [74] have prevented detailed transport and magnetisation measurements thus far. The fact that the magnitude of the diamagnetic moment is about 100 times smaller than in C_6Yb also points to reduced sample quality. We are able to conclude unambiguously that C_6Ca superconducts below 11.5K.

Figure 7d presents the magnetic phase diagram for C_6Yb inferred from magnetization measurements made with applied magnetic field in the plane of the layers (ab-

plane) and perpendicular to them (\mathbf{c}^* -axis). The lower critical field H_{C1} is approximately the same for both geometries, whilst the upper critical field H_{C2} is clearly anisotropic. The anisotropy parameter of $\Gamma_{H_{C2}}$ given by $H_{H_{C2}}(\perp_c)/H_{H_{C2}}(\parallel_c)$ is approximately 2 across the temperature range below T_{SC} . In the Ginzburg-Landau theory, this anisotropy depends solely on the ratio of the electron masses along the two symmetry directions.

Calculation of the ratio of the effective masses for pure graphite yields a value for $\Gamma_{H_{C2}}$ of 7. A comparison of these two values implies the Fermi surface is more three-dimensional in C_6Yb compared to pure graphite. This observation is consistent with normal state resistivity measurements above T_{SC} , with the measurements showing a distinct anisotropy depending on whether the current is applied in the \mathbf{c}^* -axis or in basal plane. The anisotropy can be quantified by the ratio of the \mathbf{c}^* -axis resistivity to the ab-plane resistivity, at room temperature this ratio is 100 for C_6Yb . This ratio is smaller than that in pure graphite, which at room temperature, has an anisotropy ratio [75] of around 10^4 . Further evidence for this change in Fermi surface comes from the temperature-dependent resistivity parallel to the \mathbf{c}^* -axis which reveals a significantly different behaviour from that seen in pure graphite. In pure graphite the resistivity is observed [76] to increase with decreasing temperature reaching a maximum at ~ 50 K, whilst $\rho_{\parallel c}(T)$ in C_6Yb is found to decrease from room temperature to the transition temperature. These three observations taken together lead us to believe that the Fermi surface in C_6Yb is more isotropic than that found in pure graphite.

Our results leave us with a significant question. *Is a simple charge transfer model, utilised to understand earlier studies [77,78], adequate in explaining the results reported here?* This question arises from the following observations. If charge transfer from the metal to the carbon atoms was the most important effect leading to superconductivity in these systems then we would expect C_3Li to become superconducting, since the charge transfer is comparable to that of C_6Yb and C_6Ca , with 1/3 of an electron per carbon being transferred. In fact [67] C_3Li is not superconducting. Also, in the case of C_2Li [70], where the charge transfer is greater (1/2 e per carbon), the transition temperature is still a factor of 3 and 6 smaller than in C_6Yb and C_6Ca , respectively. In the case [79] of C_2Na , which has a T_{SC} of around 5K

[78], there is no crystallographic data confirming that an ordered intercalation compound is formed. In a conventional phonon mechanism we would not expect an order of magnitude change in T_{SC} on going from a charge transfer of 1/8 of an electron per carbon to 1/3 of an electron per carbon. Therefore, our results have highlighted that there is no clear trend between the amount of charge transferred and the superconducting transition temperature. Thus, there is a demand for a renewed theoretical effort to place our findings in context with previous experimental results on the superconducting graphite intercalation compounds. In response to our discovery of superconductivity in C_6Yb and C_6Ca several new theoretical investigations have taken place [80-82]. The first of these [80] shows that superconductivity in the GIC's is always coincident with the occupation of a modified interlayer state (found in pure graphite 2 eV above the Fermi surface) and thus suggest that an acoustic plasmon mechanism may be at work. The two subsequent, and independent papers [81,82] attribute the superconductivity to the modified electron-phonon spectrum. Earlier work [83] concerning the possibility of a resonant valence bond mechanism (RVB) in the superconductivity has also been discussed in connection with these intercalation compounds. To what extent these proposals model the observed properties remains to be established.

In summary, we have synthesised two new graphite-based superconductors, C_6Yb and C_6Ca , with superconducting transition temperatures of 6.5K and 11.5K, respectively. These are unprecedented in the field of graphite intercalates. In addition, we have evidence to suggest that these compounds are more isotropic than pure graphite. This is contrary to a simple picture in which the metal atoms increase the spacing between the graphite layers; such a view would be expected to make graphite intercalants more two dimensional rather than less. In trying to understand this problem further, we will be able to exploit the weak van der Waals bonding between the graphene sheets to explore the impact of interlayer coupling using "tuning" parameters such as hydrostatic pressure or doping with different metals. In addition, this work may also be of more general importance in understanding and exploring superconductivity in the quasi-one dimensional system formed in single walled carbon nanotubes [84].

References

1. N Doiron-Leyraud, et al., *Nature* **425** (2003) 595.
2. K G Sandeman, G G Lonzarich and A J Schofield, *Phys. Rev. Lett.* **90** (2003) 167005.
3. P Monthoux and G G Lonzarich. submitted to *Phys. Rev. B* (2003); *Phys. Rev. B* **66** (2002), **63** (2001), **59** (1999); P Monthoux, *Phys. Rev. B* **68** (2003) 064408.
4. F Nakamura, et al., *Phys. Rev. B* **65** (2002) 220402.
5. D Forsythe, et al., *Phys. Rev. Lett.* **89** (2002) 166402.
6. I H Inoue, et al, *Phys. Rev. Lett.* **88** (2002) 236403.
7. A J Millis, et al., *Phys. Rev. Lett.* **88** (2002) 217204.
8. L Capogna, et al., *Phys. Rev. Lett.* **88** (2002) 076602.
9. S A Grigera, et al., *Science*, **294** (2001) 329 to be published.
10. R B Laughlin, et al., *Adv. in Phys.* **50** (2001) 361.
11. R S Perry, et al., *Phys. Rev. Lett.* **86** (2001) 2661.
12. C Pfleiderer, S R Julian and G G Lonzarich, *Nature*, **414** (2001) 427.
13. C Pfleiderer, et al., *Nature*, **412** (2001) 58.

14. C Bergemann, et al., *Phys. Rev. Lett.* **84** (2000) 2662.
 15. F M Grosche, et al., *J. Phys-Cond. Mat.* **12** (2000) L533.
 16. S S Saxena, et al., *Nature*, **406** (2000) 587; S S Saxena and P B Littlewood, *Nature*, **412** (2001) 290.
 17. I R Walker, *Rev. Sci. Instr.* **70** (1999) 3402.
 18. A P Mackenzie, et al., *Phys. Rev. Lett.* **80** (1998) 161.
 19. N D Mathur, et al., *Nature*, **394** (1998) 39.
 20. G G Lonzarich in *Electron* (1997) and *Electrons on the Fermi Surface* (1980), ed. Springford M (Cam. U. Press).
 21. C Pfleiderer, et al., *Phys. Rev. B* **55** (1997) 8330.
 22. S R Julian, et al., *J. Phys-Cond. Mat.* **8** (1996) 9675.
 23. A P Mackenzie, et al., *Phys. Rev. Lett.* **76** (1996) 3786.
 24. S R Julian, et al., *Physica B* **199 & 200** (1994) 63.
 25. A P Mackenzie, et al., *Phys. Rev. Lett.* **71** (1993) 1238.
 26. S R Julian, et al., *Phys. Rev. B* **15** (1992) 9821.
 27. N R Bernhoeft, et al., *Phys. Rev. Lett.* **62** (1989) 657.
 28. L Taillefer and G G Lonzarich, *Phys. Rev. Lett.* **60** (1988) 1570; S M Hayden, et al, *Phys. Rev. B* **33** (1986) 4977.
 29. G G Lonzarich and L Taillefer, *J. Phys. C* **18** (1985) 4339.
 30. H Yuan, D Jaccard, K Miyake, private communications.
 31. T Moriya, *Acta Phys. Pol. B* **34** (2003) 287.
 32. N Tateiwa, et al., *Acta Phys. Pol. B* **34** (2003) 515.
 33. MJ Bull, et al., *Acta Phys. Pol. B* **34** (2003) 1265.
 34. YA Timofeev, et al., *Rev. Sci. Instru.* **73** (2002) 371.
 35. P Coleman, Lecture Notes, ICTP, Trieste (2002).
 36. A Demuer, et al., *J. Phys-Cond. Mat.* **14** (2002) L529.
 37. S Kawasaki, et al., *Phys. Rev. B* **66** (2002) 054521; **65** (2002) 020504
 38. G Knebel, et al., *High Pres. Res.* **22** (2002) 167.
 39. J R Stewart, et al., *Phys. Rev. Lett.* **89** (2002) 186403.
 40. D Aoki, et al., *Nature*, **413** (2001) 613.
 41. K Shimizu, et al., *Nature*, **412** (2001) 316.
 42. G Chapline, et al., *Phil. Mag.* **B 81** (2001) 235 to be published.
 43. Y Maeno, T M Rice and M Sigrist, *Phys Today* (1/2001) 42; C Honerkamp and T M Rice, *Physica C* **388-9** (2003) 11.
 44. F Steglich, *J Magn. Magn. Mater.* **226** (2001) 1.
 45. A Schroder, et al., *Nature*, **407** (2000) 351.
 46. D Belitz, et al., *Phys. Rev. Lett.* **85** (2000) 4602.
 47. H Hegger, et al., *Phys. Rev. Lett.* **84** (2000) 4986.
 48. H M Ronnow, et al., *Physica B* **276-278** (2000) 676.
 49. R J Beynon and J Wilson, *J. Phys-Cond. Mat.* **5** (1993) 1983.
 50. Y Onishi and K Miyake, *J. Phys. Soc. Jpn.* **69** (2000) 3955.
 51. A J Millis, *Phys. Rev. B* **48** (1993) 7183.
 52. P Monthoux and D Pines, *Phys. Rev. B* **47** (1993). 6069; S Nakatsuji, D Pines and Z Fisk, *Cond-Mat/0304587*.
 53. D Jaccard, et al., *Phys Lett.* **163A** (1992) 475.
 54. G Baym and C Pethick, Ch. 3 in *Landau Fermi-liquid theory* (1991, Wiley).
 55. J A Hertz, *Phys. Rev. B* **14** (1976) 1165.
 56. T Moriya and A Kawabata, *J. Phys. Soc. Jpn* **34** (1973) 639.
 57. K K Murata and S Doniach, *Phys. Rev. Lett.* **29** (1972) 285.
 58. S Q Wang, W E Evenson and J R Schrieffer et al., *Phys. Rev. Lett.* **23** (1969) 92.
 59. D M Edwards and E P Wohlfarth, *Proc. R. Soc. A* **303** (1968) 127.
 60. S M Hayden, private communications.
 61. T E Weller, M Ellerby, S S Saxena, R P Smith and N T Skipper, *Nature Physics*, **1** (2005) 39.
 62. G Cyani, *Nature Physics*, **1** (2005) 42.
 63. G Chaplain, Private Communication, June 2004.
 64. P Coleman and A Schofield, *Nature*, (2005).
 65. M S Dresselhaus and G Dresselhaus, *Advances in Physics*, **51** (2002) 1-186.
 66. H Zabel and S A Solin, Springer-Verlag: Berlin (1990, 1992).
 67. T Enoki, S Masatsugu and E Morinobu, OUP: Oxford (2003).
 68. N B Hannay, Geballe et al., *Phys. Rev. Lett.* **14** (1965) 225-226.
 69. Y Koike, et al., *Physica B+C*, **99** (1980) 503-508.
 70. I T Belash, et al., *Solid State Commun.* **69** (1989) 921-923.
 71. E I Makrini, et al., *Physica*, **99 B** (1980) 481-485.
 72. N Emery, et al., <http://xxx.soton.ac.uk/ftp/cond-mat/papers/0506/0506093.pdf> (June 2005).
 73. R M Moon, et al., *Phys. Rev.* **176** (1968) 722-731.
 74. D Guérard, et al, *Carbon.* **18** (1980) 257-264.
 75. Kopelevich, et al., *Phys. Rev. Lett.* **90 15** (2003) 156402/1-4.
 76. Uher, et al., *Phys. Rev B* **35** (1987) 4483-4488.
 77. R Al-Jishi, et al., *Phys. Rev. B* **44** (1991) 10248-10255.
 78. Al-Jishi, et al., *Phys. Rev. B* **45** (1992) 12465-12469.
 79. I T Belash, et al., *Solid State Commun.* **64** (1987) 1445-1447.
 80. G Cs'anyi, et al., http://xxx.soton.ac.uk/PS_cache/cond-mat/pdf/0503/0503569.pdf (Mar 2005).
 81. I I Mazin, http://xxx.soton.ac.uk/PS_cache/cond-mat/pdf/0504/0504127.pdf (April 2005).
 82. M Calandra, et al., http://xxx.soton.ac.uk/PS_cache/cond-mat/pdf/0506/0506082.pdf (June 2005).
 83. G Baskaran, et al., *Phys. Rev. B* **65** (2002) 212505/1-4.
 84. S Suzuki, et al., *Phys. Rev. B* **67** (2003) 115418 /1-6.
- A substantial part of the work mentioned here was performed in the Low Temperature Physics Group in the Cavendish under the guidance of Prof. G. G. Lonzarich, FRS and the colleagues mentioned in specific references, particularly Refs. 16th and 19th.
- Regarding Graphite and Ferroelectric work we also acknowledge M. Baxendale and M. Laad for their fruitful comments, suggestions and discussions. In the preliminary development of the graphite sample

preparation we are indebted to C. Gallagher, J. Goodyer and S. L. Molodtsov (Dresden TU). We thank K.S. Lee (London Centre for Nanotechnology UCL) and Institute of Archaeology, UCL for SEM-EDAX studies on the final samples. We are also grateful to the Eastman Dental Institute for cutting of graphite samples. We are thankful to G. Aepli, G. Cs'anyi, A.H. Harker, A. Kusmartseva, N. D. Mathur, D.F. McMorrow, F.

Morrison, A. H. Nevidomskyy, C. Pickard, P.B. Littlewood, J. Loram, S. Özcan, Ch. Renner, S. Rowley, J. F. Scott and B.D. Simons for useful discussions. We would also like to thank the EPSRC, CCLRC (ISIS), The Royal Society, Jesus and Trinity Colleges of the University of Cambridge for financial support. Correspondence and requests for materials should be addressed to Dr. S.S. Saxena (e-mail: sss21@cam.ac.uk)

Archive of SID